Updates on bendamustine metabolites in plasma and excreta of sprague dawley rats and cynomolgus monkeys.

Li AC*, Erya Yu, Ring SC, Chovan JP

Drug Metabolism and Pharmacokinetics, Teva Pharmaceuticals Specialty R&D, Inc., West Chester, PA 19380, USA

Abstract

A derivative of bendamustine, designed for longer duration of activity and better distribution into tissues, was intravenously infused to rats and monkeys. The parent BM derivative was rapidly metabolized in both species. Consequently, BM and BM-related metabolites were essentially all that were detected and identified from plasma and excreta of both species. A variety of new metabolites have been identified, including 5 intact direct conjugates of glutathione, 2 cysteinyl-glycine conjugates, 1 glucuronic acid conjugate, and 1 taurine conjugate on the butyric acid side, in addition to a new metabolite of an aziridine partial structure formed due to N-dealkylation and intra-molecular nucleophilic/electrophilic reaction. The overall biotransformation pathways are similar to those previously reported, including substitution of the chlorine atoms (glutathione, cysteinyl-glycine, mercapturic acid, hydroxyl, creatinine, uric acid and phosphate), N-dealkylation to cleave the chloroethyl moiety, and γ-hydroxylation on the butyric acid moiety. However, new biotransformation pathways have been discovered in the current work, unrelated to the derivatization of the parent compound, which includes phase II conjugation on the butyric acid with glucuronic acid and taurine in rat, and a proposed intra-molecular nucleophilic/electrophilic mechanism in monkey. No metabolite due to the previously reported N-demethylation was detected from either species in the current study. In addition, based on exact mass measurements of both survey full scan and dependent product ion data, an imine structure is presented instead of an aldehyde structure that was proposed previously, and another metabolite has been postulated to have a carboxylic acid functionality on the original chloroethyl moiety.

Keywords: Bendamustine, Hydrogen-Deuterium Exchange (HDX), Glutathione (GSH).

Accepted on April 11, 2018

Introduction

The alkylating agent bendamustine (Figure 1) has been clinically used for over 30 years in Germany and was approved in 2008 by the U.S. Food and Drug Administration for the treatment of patients with chronic lymphocytic leukemia (CLL) and rituximab-refractory, indolent B cell non-Hodgkin's lymphoma. In order to improve the half-life and/or biodistribution of BM, a new formulation has been developed using proprietary nanoparticle technologies and a derivative of BM has been identified as the optimal candidate for drug loading and improved distribution. In preparation for human studies, the compound was dosed to rat and monkey to obtain metabolism and disposition information. However, because of proprietary reasons, the structure of the derivative is not presented in this report. As will be shown, essentially all the derivatives detected are unrelated to the metabolism of the parent BM derivative, which is rapidly converted to BM *in vivo* in both species.

The *in vivo* metabolic profile of BM has been reported previously not only by this laboratory [1], but also by other investigators [2-4]. The biotransformation pathways included γ-hydroxylation on the butyric acid moiety, N-demethylation on the benzimidazole heterocyclic ring, N-dealkylation to truncate the chloroethyl moieties and substitution of the chlorine atoms with nucleophilic functionalities, such as hydroxyl, cysteine derivatives, creatinine, uric acid, and phosphate. Sulfoxides of BM mercapturates were also identified [2]. This study was to obtain metabolism and disposition information of this BM derivative, particularly to investigate whether there is a major difference in biotransformation in comparison with that of BM. This information is also necessary in preparation for the conduct of clinical studies. In our investigation of the metabolism of the BM derivative, the overall metabolic profile was found to be similar to that were reported previously for BM, but several new metabolites have been detected. Two phase II conjugates of the carboxylic acid side were discovered, in addition to new parent BM metabolites that were not reported. Furthermore, based on exact mass measurements, a revised structure proposal is presented herein for the metabolite that had a m/z of 276 $[M + H]^+$.

Materials and Methods

Reference standards and chemicals

Reference standards of bendamustine (4-[5-[bis(2-chloroethyl) amino]-1-methyl-benoimidazol-2-yl] butyric acid; MW 357), its derivative, and γ-hydroxy-bendamustine (M276) were synthesized by Teva Branded Pharmaceutical Products R&D, Inc. (West Chester, PA, USA). The 14C-labeled BM derivative (radiochemical and chemical purity >99%) was synthesized by Quotient Bioresearch Ltd. (Cardiff, UK). The non-labeled BM

derivative was used for diluting the radiolabeled material to reduce the specific activity of the formulated dose. The mixture of labeled and non-labeled compound was prepared using a proprietary procedure and lyophilized prior to resuspension in normal saline for dosing. Ammonium acetate and HPLC-grade acetonitrile (ACN) and formic acid were all from Sigma-Aldrich Chemical Company, St. Louis, MO, USA or VWR International, West Chester, PA, USA. Purified water was obtained from an in-house Milli-Q ultrapurification system (Millipore, Billerica, CT, USA). Deuterium oxide (D_2O) was purchased from Cambridge Isotope Laboratories, Inc., Cambridge, MA, USA.

Samples

Rats and monkeys were administered intravenous 30 minute infusions of the formulated BM derivative at 15.5 and 4.33 mg/kg, respectively. Rat bile and urine samples were collected on wet ice at selected times after the infusion and were analyzed immediately after collection so as to reduce the possibility of metabolite degradation. Feces samples from rat were transferred to dry ice and then stored at -80°C until prepared for analysis. Monkey urine and feces were collected on dry ice and stored in -80°C pending analysis. Plasma samples were pooled according to post dose time points and were extracted by mixing with 3 volumes of ACN. The mixture was then centrifuged at 14000 g for 10 min. The supernatant was removed, evaporated, and reconstituted in starting HPLC mobile phase for analysis. Feces samples were homogenized in 3-volumes of methanol 3 times. The supernatants were combined, evaporated to small volumes, and reconstituted in methanol: water (1:1) for analysis.

Metabolite detection

Metabolites were detected by an online HPLC-MS-radioactivity detector data collection system. A Shimadzu Prominence HPLC system (Kyoto, Japan) was used with a Phenomenex Synergi Hydro-RP column (Phenomenex, Palo Alto, CA, USA). The effluent was split 3/7 between a ThermoFisher Scientific linear ion trap LTQ-Orbitrap mass spectrometer (Thermo Scientific, Somerset, NJ, USA) (electrospray, positive ion mode) and a model 4 IN/US β-Ram radioactivity detector (LabLogic, Brandon, FL, USA), respectively. The response from the latter detector, in mV, was collected by the Xcalibur software. This software also integrated the peaks of radioactivity; the total area of the integrated peaks in a chromatogram was then used to estimate the percent of the amount of injected radioactivity contained in a particular peak.

Analytes were eluted from the column with 5 mM ammonium acetate in water (A) and acetonitrile (B). The stepwise linear gradient was 0% B isocratic (0-3 min), 0-30% B (3-16 min), 30-90% B (16-18 min), 90% B isocratic (18–24 min), returning to 0% B in 0.5 min). The column was re-equilibrated for 5.5 min prior to the next injection; hence, the total run was 30 min. The column temperature was controlled at 35°C. For hydrogen-deuterium exchange (HDX) runs, D_2O was used to replace H_2O in the preparation of mobile phase A. The total mobile phase flow rate was set at 1.0 mL/min and was split post column so to let ~300 µL/min go to the mass spectrometer, and ~700 µL/min go to the radiochemical detector where the flow was mixed with scintillation liquid at 1.05 mL/min for radioactivity monitoring. The mass spectrometer was tuned to optimal conditions for BM and was operated under a data-dependent acquisition mode, which consisted of a survey full scan (100–1000 m/z) at a resolution of 30 K and up to 4 dependent product ion scans at a resolution of 7.5 K.

Metabolite identification

Ions detected in the survey scan that also corresponded to a radiochemical chromatographic peak were examined according to the following:

1. **Biotransformation knowledge-based prediction or calculation for possible metabolites:** Metabolites were predicted based on the possible phase I biotransformation of the derivative and BM and in combination with direct or phase II conjugation.

2. **Isotopic pattern:** If an ion showed an isotope pattern of chlorine, the ion could be likely related to the dosed compound or BM.

3. Mass defect: Visual inspection of the mass defect of an ion detected in the accurate mass measurement survey scan could quickly lead to the inclusion or exclusion of possible metabolites.

4. Product ions that were common to BM or known metabolites: If an ion generated product ions that were shared by BM and/or known metabolites of BM, the ion was then highly regarded as a metabolite. This is particularly convincing given the exact mass measurements of the product ions.

5. Confirmation by analysis of mass spectrometric fragmentation and hydrogen-deuterium exchange (HDX): Confirmation by analysis of mass spectrometric fragmentation and hydrogen-deuterium exchange leading to structure proposals.

Results

The metabolites were designated according to their protonated molecular weights. Thus, since the m/z ($[M+H]^+$) of hydroxylated BM would be m/z 374, the metabolite will be named as M374. However, in the current naming system, retention time is still used to distinguish metabolites that have the same protonated mass, such as M472A and M472B.

Metabolites in rat excreta

The dosed BM derivative was not detected in any rat sample. Most of the rat metabolites were observed in bile samples, as shown in the radio chromatogram of Figure 2A. The MS survey scan revealed additional metabolites. A total of 24 metabolites were detected in the bile sample. Analysis of rat urine samples (Figure 2B) revealed 13 metabolites, 6 of which were detected in bile. Plasma sample radio chromatograms showed only baseline radioactivity by the online analysis, but 8 metabolites were detected by the mass spectrometer. M276 and M296 were detected along with 3 unknown metabolites (M368, M352, and M382) from rat feces (Figure 2C). All metabolites are listed in Table 1.

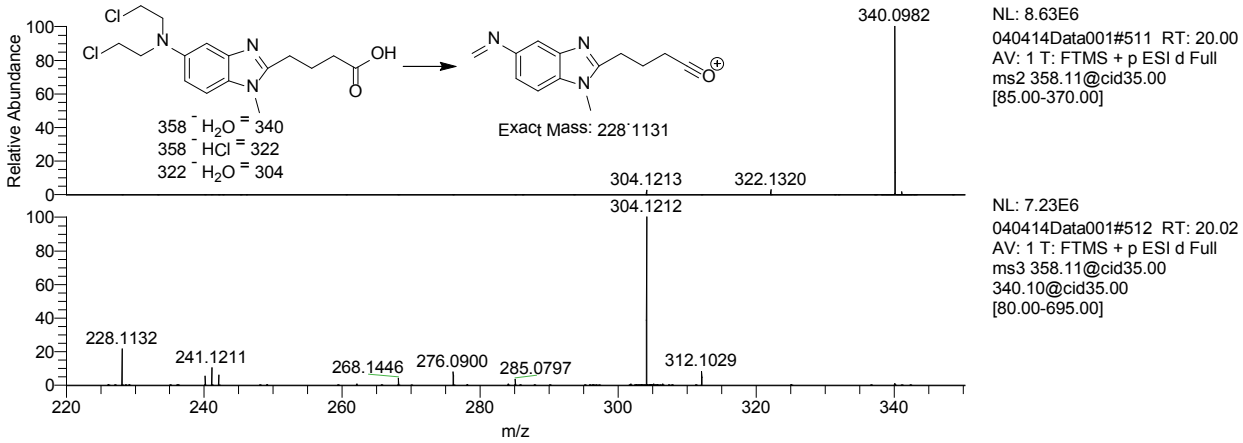

Figure 1. *Chemical structure and mass spectrometric fragmentation of bendamustine.*

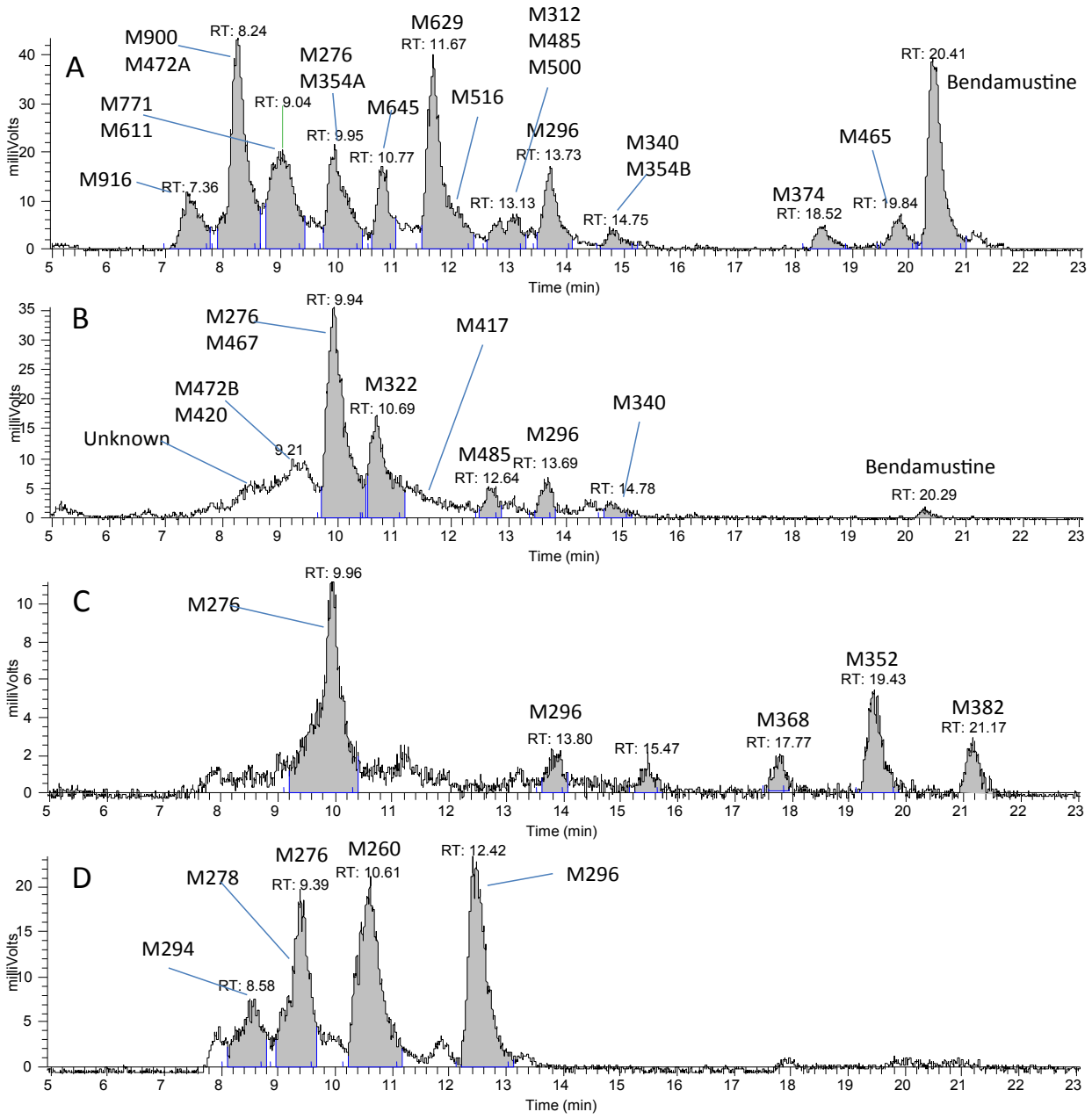

Figure 2. *Radiochemical profile of bendamustine metabolites in (A) rat bile (B) Rat urine (C) Rat feces and (D) Monkey urine* [Note: Significant retention time shift in monkey urine analysis (D) due to the use of a different column].

Table 1. *Overview of structural information obtained by LC-MSn for bendamustine metabolites detected in rat and monkey plasma and excreta.*

Metabolites	T_R (min)	$[M + H]^+$		Proposed Formula	Δ ppm	Proposed Biotransformation		
		Measured	Theoretical			Chloroethyl-1	Chloroethyl-2	Butyric acid
M916	7.36	916.3186	916.3175	$C_{36}H_{54}N_9O_{15}S_2$	1.2	GSH conj.	GSH conj.	hydroxylation
M336	7.76	336.1552	336.1554	$C_{16}H_{22}N_3O_5$	-0.6	OH replaced Cl	carboxylic acid	Intact
M472A	8.24	472.1481	472.1481	$C_{20}H_{27}ClN_3O_8$	-0.1	N-dealkylated	Intact	glucuronide conj.
M900	8.25	900.3233	900.3226	$C_{36}H_{54}N_9O_{14}S_2$	0.7	GSH conj.	GSH conj.	Intact
M292A	8.33	292.1291	292.1292	$C_{14}H_{18}N_3O_4$	-0.2	N-dealkylated	carboxylic acid	Intact
M771	8.86	771.2805	771.2800	$C_{31}H_{47}N_8O_{11}S_2$	0.6	GSH conj.	Cys-Gly conj.	Intact
M292B	8.86	292.1291	292.1292	$C_{14}H_{18}N_3O_4$	-0.2	N-dealkylated	imine or aldehyde	hydroxylation
M294	9.01	294.1268	294.1271	$C_{14}H_{20}N_3O_2S$	-0.8	SH replaced Cl	N-dealkylated	Intact
M612	9.02	612.2152	612.2156	$C_{26}H_{38}N_5O_8S_2$	-0.7	mercapturate conj.	mercapturate conj.	Intact
M611	9.04	611.2494	611.2494	$C_{26}H_{39}ClN_6O_9S$	0.0	GSH conj.	OH replaced Cl	Intact
M278	9.13	278.1497	278.1499	$C_{14}H_{20}N_3O_3$	-0.8	OH replaced Cl	N-dealkylated	Intact
M472B	9.21	472.1941	472.1939	$C_{21}H_{26}N_7O_6$	0.3	creatinine conj.	OH replaced Cl	Intact
M420	9.33	420.1088	420.1086	$C_{16}H_{24}ClN_3O_6P$	0.6	phosphate replaced Cl	Intact	Intact
M467	9.90	467.1959	467.1959	$C_{21}H_{31}N_4O_6S$	0.0	mercapturate conj.	OH replaced Cl	Intact
M276	9.94	276.1344	276.1343	$C_{14}H_{18}N_3O_3$	0.5	OH replaced Cl, imine	N-dealkylated	Intact
M354A	9.95	354.1216	354.1215	$C_{16}H_{21}ClN_3O_4$	0.3	OH replaced Cl	carboxylic acid	Intact
M260	10.55	260.1392	260.1394	$C_{14}H_{18}N_3O_2$	-0.5	dechlorinated, aziridine	N-dealkylated	Intact
M322	10.6	322.1761	322.1761	$C_{16}H_{24}N_3O_4$	0.0	OH replaced Cl	OH replaced Cl	Intact
M645	10.77	645.2109	645.2104	$C_{26}H_{39}ClN_6O_9S$	0.7	GSH conj.	Intact	hydroxylation
M501	11.28	501.1564	501.1569	$C_{21}H_{30}ClN_4O_6S$	-1.0	mercapturate conj.	Intact	hydroxylation
M629	11.67	629.2158	629.2155	$C_{30}H_{25}F_2N_4O_9S$	0.5	GSH conj.	Intact	Intact
M417	11.75	417.2247	417.2245	$C_{20}H_{29}N_6O_4$	0.5	uric acid conj.	OH replaced Cl	Intact
M516	12.02	516.1676	516.1678	$C_{21}H_{31}ClN_5O_6S$	-0.3	Cys-Gly conj.	Intact	hydroxylation
M312	13.05	312.1110	312.1110	$C_{14}H_{19}ClN_3O_3$	0.3	N-dealkylated	Intact	hydroxylation
M485	13.10	485.1619	485.1620	$C_{21}H_{30}ClN_4O_5S$	-0.1	mercapturate conj.	Intact	Intact
M500	13.14	500.1727	500.1729	$C_{21}H_{31}ClN_5O_5S$	-0.4	Cys-Gly conj.	Intact	Intact
M443	13.19	443.1512	443.1514	$C_{19}H_{28}ClN_4O_4S$	-0.6	Cys conj.	Intact	Intact
M296	13.73	296.1163	296.1160	$C_{14}H_{19}ClN_3O_2$	0.9	N-dealkylated	Intact	Intact
M340	14.75	340.1423	340.1423	$C_{16}H_{23}ClN_3O_3$	0.2	OH replaced Cl	Intact	Intact
M354B	14.80	354.1215	354.1215	$C_{16}H_{21}ClN_3O_4$	-0.1	OH replaced Cl	OH replaced Cl, amide	Intact
M435	16.22	435.1907	435.1906	$C_{20}H_{28}ClN_6O_3$	0.2	uric acid conj.	Intact	Intact
M374	18.52	374.1030	374.1033	$C_{16}H_{22}Cl_2N_3O_3$	-0.6	Intact	Intact	hydroxylation
M465	19.84	465.1123	465.1125	$C_{18}H_{27}Cl_2N_4O_4S$	-0.5	Intact	Intact	taurine conj.
Bendamustine	20.41	358.1081	358.1084	$C_{16}H_{22}Cl_2N_3O_2$	-0.6	Intact	Intact	Intact

Notes: 1. Δ ppm = [(Measured mass – Theoretical mass) × 1000 × 1000/Theoretical mass];
2. Theoretical mass: Generated by ChemDraw Ultra 11.0.1, Cambridge Soft

Metabolites in monkey excreta

The BM derivative was only detected in early samples (0.5–0.75 hr from start of infusion) of monkey plasma, along with M276, M260 and M296. Monkey urine (Figure 2D) showed the presence of M294, M276, M278, M260 and M296. Similar to rat feces, 2 unknown metabolites, M368 and M352, were also detected, along with M276 and M296.

Metabolite identification

Although BM metabolites have been well documented in recent years, the current work still revealed some new metabolites. This communication will focus on the new metabolite identification and update the proposal for the metabolites that were reported previously by this laboratory with new, accurate mass data. Since BM was used as the reference compound for the identification of metabolites, its product ions and fragmentation interpretation are presented in Figure 1.

M900, observed in rat bile, had a chromatographic retention time of 8.25 min. The survey scan exact mass and the dependent mass fragmentation (Table 2 and Scheme 1) proved that M900 was a conjugate of BM with 2 glutathione units. Due to the lack of chlorine isotope pattern, M900 must be formed by substitution of the 2 chlorine atoms with glutathione moieties.

M916 eluted earlier (7.36 min) than M900, and the product ion spectrum (Table 2 and Scheme 1) resembled that of M900 except that all ions were 16 Da higher than the counterpart ions of M900. Therefore, M916 was proposed as di-glutathione conjugate of hydroxylated BM. Since γ-hydroxylation was reported previously (so-called M3) and detected in the current work (M374), the hydroxylation in M916 was also proposed to be at the γ-position on the butyric acid moiety.

M336 in rat bile also lost the chlorine isotope pattern. The elemental composition based on exact mass measurement suggested that a new carbonyl functionality was formed in the metabolite structure. The ion transition m/z 318 → m/z 260 in mass fragmentation

Table 2. *MS fragment ions of bendamustine and its metabolites detected in rat and monkey plasma and excreta.*

Compounds	MS^2	MS^3
M916	898.3082, 787.2762, 769.2651, **658.2329**	**640.2224**, 622.2154, 514.1787, 454.1752, 436.1655
M336	**318.1451**, 290.1501, 277.1423	300.1341, 274.1552, 272.1033, **260.1394**, 246.1602, 228.1132, 217.0973
M472A	454.1381, 392.1376, 368.1272, **296.1165**	**278.1060**, 262.1678, 203.0999
M900	882.3101, 771.2803, 753.2691, **642.2375**	**624.2272**, 498.1841, 438.1805
M292A	**274.1190**, 256.1083	**256.1083**, 228.1130
M771	753.2711, **642.2391**	**624.2274**, 498.1840, 438.1806, 420.1706
M292B	**274.1188**, 256.1080	**256.1082**, 232.1079, 203.0523
M294	**276.1169**	**248.1215**, 242.1288, 229.1205, 221.0980, 214.0974
M611	593.2396, **482.2072**, 338.1540	464.1967, 338.1538, **278.1501**, 177.0329
M276	**258.1238**	**230.1290**, 217.0974, 203.1053
M354A	**336.1115**, 308.1166, 295.1090	308.1165, 292.1218, **278.1060**, 256.1450, 228.1135
M260	**242.1290**, 240.1135, 214.1340	227.1054, **214.1339**, 212.1183, 187.1104
M645	627.1997, **516.1675**	**498.1565**, 480.1476, 312.1108, 177.0327
M501	**483.1462**, 372.1145, 312.1111, 296.1006, 162.0220	354.1033, **294.1003**, 162.0217
M629	611.2051, **500.1730**	**482.1619**, 356.1194, 296.1161, 177.0328
M516	**498.1574**, 480.1484, 312.1113, 177.0330	**480.1466**, 352.0890, 294.1008, 177.0327
M500	482.1630, 357.2289, **296.1166**, 278.1060, 177.0331, 162.0222	NA
M354B	296.1164, **278.1059**	263.0822, 250.1108, **242.1290**, 223.0871, 214.0975
M465	429.1361, **340.0981**	312.1031, **304.1215**, 276.0902, 228.1134
Bendamustine	**340.0982**, 322.1320, 304.1213	312.1029, **304.1212**, 276.0900, 241.1211, 228.1132

Notes: 1. Fragment ions in bold represent base peak; 2. Base peak in MS^2 triggered MS^3 acquisition.

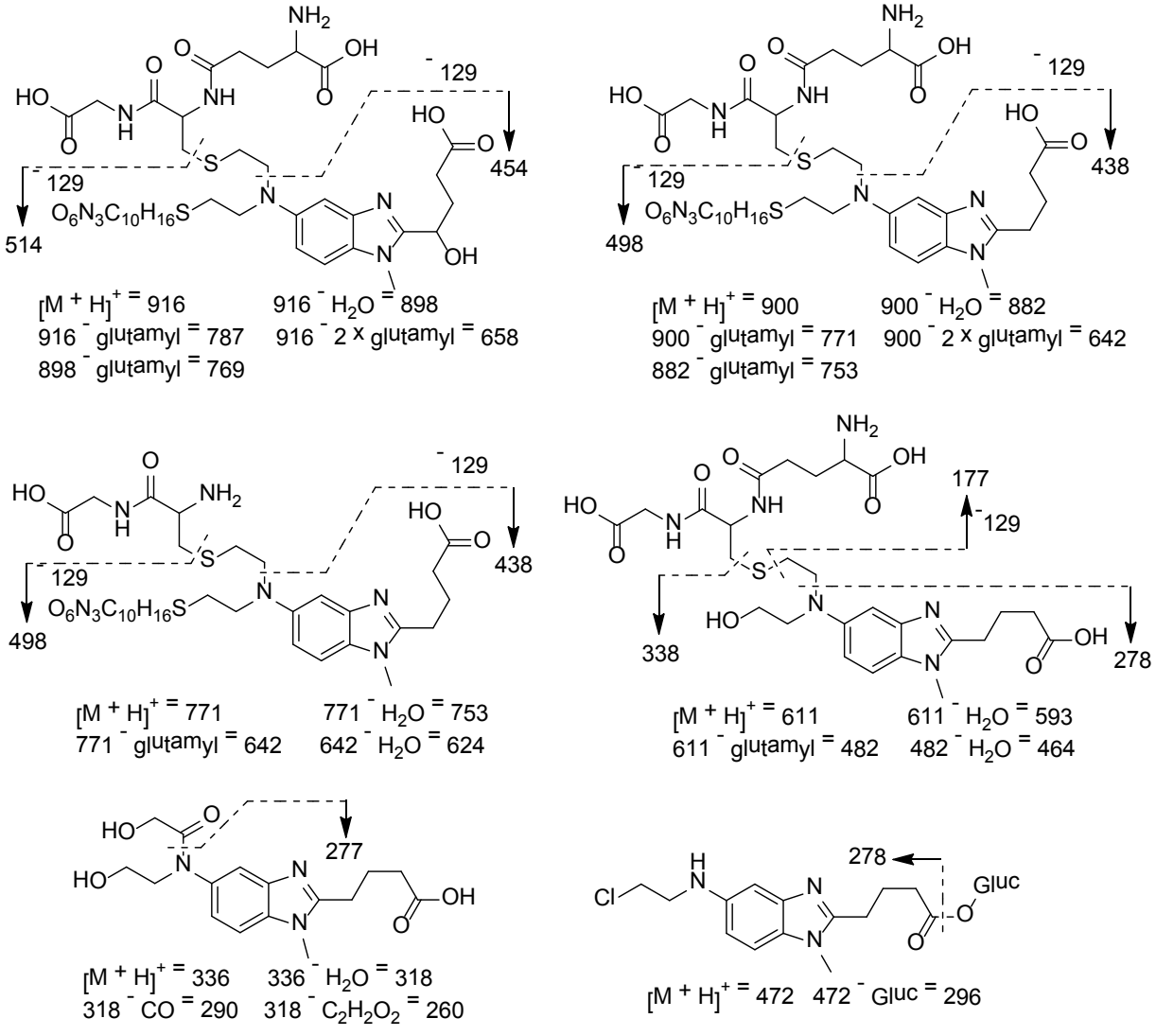

Scheme 1. *Proposed mass spectrometric fragmentation pathways of M916, M900, M771, M611, M336 and M472A.*

indicated that this carbonyl was adjacent to the amino nitrogen atom and so facilitating α-cleavage (Table 2 and Scheme 1).

The survey scan data for M472A from rat bile indicated that the metabolite still retained one chlorine atom. Calculation of theoretical mass resulted in the proposal for M472A as a glucuronide conjugate of des-chloroethyl BM, which was in agreement with the product ion shown in Table 2 and Scheme 1.

The survey scan data indicated M771 lost the chlorine isotope pattern. The neutral loss of 129 Da in fragmentation (Table 2 and Scheme 1) proved that this metabolite was a glutathione conjugate. Calculation of exact mass led to the proposal of an additional cysteinyl-glycine moiety in the structure.

M611 from rat bile underwent a neutral loss of 129 Da in the fragmentation (Table 2 and Scheme 1), proving that this metabolite was a glutathione conjugate. Further MS data analysis led to the rationalization of the M611 structure to be the result of substitution of the chlorine atoms by glutathione and hydroxyl.

M292A and M292B were reported previously by this laboratory. With exact mass measurements (Tables 1 and 2), the product ion m/z 228 of M292A seemed to indicate that a carboxylic acid functionality formed on the original chloroethyl moiety (Scheme 2). Yet, the structure of M292B still remains ambiguous, even though the hydroxylation was postulated on the γ-position of the butyric acid moiety. The double bond could be in the form of either an aldehyde or an imine on the ethylamine moiety, which could both satisfy the requirement of increasing 4 Da in the HDX analysis.

M294 from monkey urine also lost the chlorine isotope pattern. The exact mass measurement of the protonated M294 corresponded well with a thiol substitution of chlorine for a des-chloroethyl BM (Tables 1 and 2).

Previously, this laboratory postulated M276 with an aldehyde partial structure. The exact mass measurement in current work provided evidence that the metabolite might have an imine structure. As shown in Table 2 and Scheme 2, if the product ion m/z 258 was solely formed by losing water from the carboxylic acid group, it would be impossible to generate the ion (MS3) m/z 217. Therefore, the precursor ion (m/z 258) for the MS3 product ion m/z 217 had to be generated (MS2) by losing a water molecule on the ethylamine moiety. Hence, the product ion (MS2) m/z 258 must be a mixture of two isomeric ions, due to the loss of water from the carboxylic acid on the butyric acid moiety and a hydroxyl group on the ethylamine moiety, respectively. To maintain such a hydroxyl group, an imine structure was rationalized on the ethylamine moiety to satisfy both the product ion (MS3) m/z 217 and the HDX result. The metabolite increased 3 m/z units in HDX analysis, indicating the metabolite had 2 exchangeable hydrogen atoms besides the charge.

The isomeric M354A and M354B were both detected in rat bile. They had a nearly 5-minute difference in retention times under the current chromatographic conditions. They also showed different fragmentation, as shown in Table 2. The ion transitions m/z 336 → m/z 256 (loss of HCl and CO_2) and m/z 336 → m/z 228 (loss of chloroethane and CO_2) of M354A both indicated that the metabolite had a second carboxylic acid

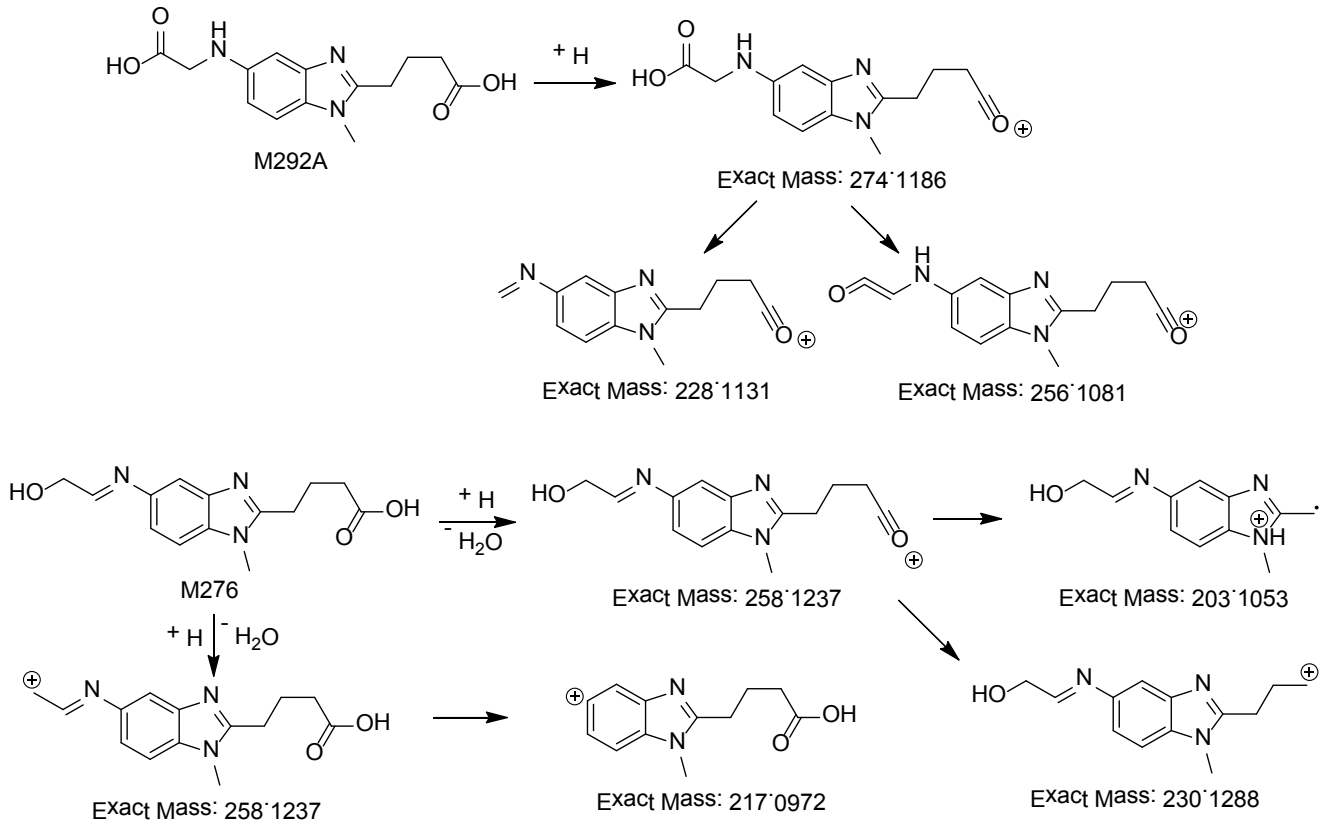

Scheme 2. *Proposed mass spectrometric fragmentation pathway of M292A and M276.*

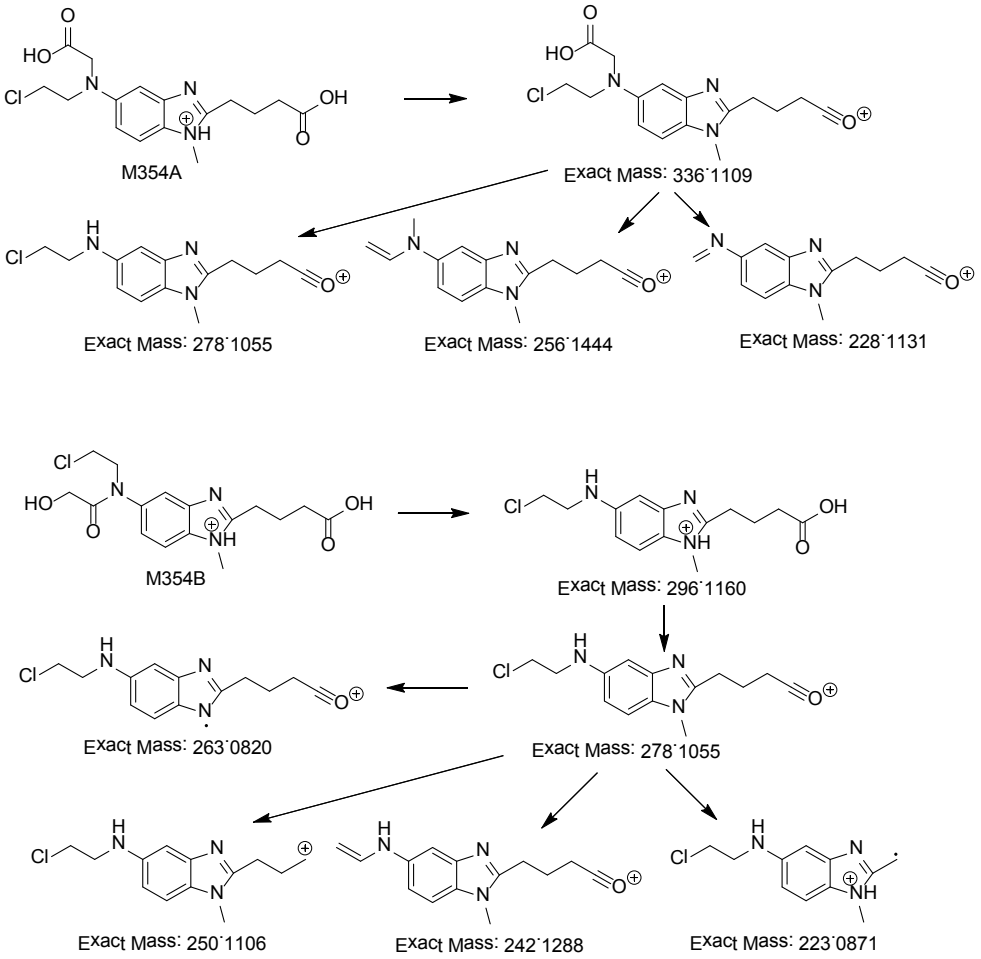

Scheme 3. *Proposed mass spectrometric fragmentation pathway of M354A and M354B.*

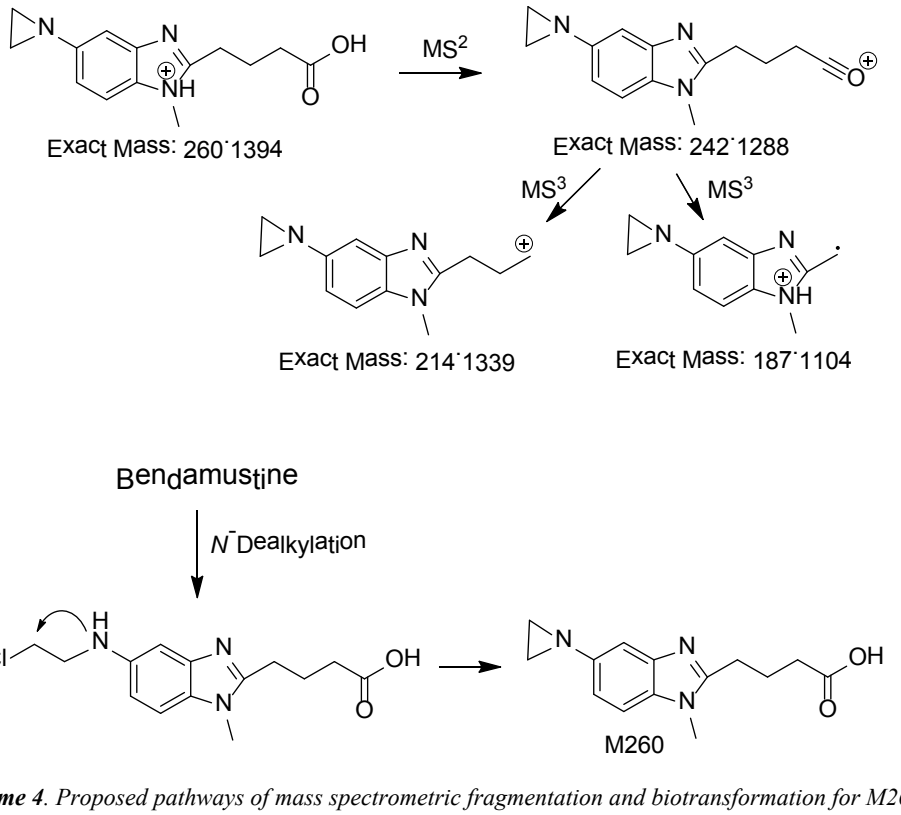

Scheme 4*. Proposed pathways of mass spectrometric fragmentation and biotransformation for M260.*

functionality in addition to the butyric acid moiety. Since the original butyric acid moiety did not undergo such a neutral loss of CO_2 as observed from the fragmentation of BM (Figure 1), the additional carboxylic acid group in M354A was assigned on the ethane moiety. Therefore, the structure of M354A was postulated based on the rationalization shown in Scheme 3. On the other hand, M354B did not undergo the neutral loss of CO_2, but a neutral loss of 58 Da to generate product ions m/z 296 (loss of COCHOH) and m/z 278 (loss of COCHOH and H_2O, 76 Da). Hence, M354B was rationalized to have an amide partial structure as shown in Scheme 3.

M260 was observed in monkey urine and plasma and did not show a characteristic chlorine isotope pattern. The mass fragmentation (Scheme 4) implied that the butyric acid moiety was not altered; hence, the structure modification was postulated to be an aziridine formation out of combined consideration of the measured exact mass in survey scan, the HDX result (a 2-Da increase), and possible biotransformation mechanism. The latter could be the nucleophilic attack of the nitrogen to the electrophilic carbon atom adjacent to the chlorine atom (Scheme 4).

M645, M501, and M516 all showed a characteristic isotope pattern for 1 chlorine atom in survey scan data. This indicated that the other chlorine atom was replaced by components with larger masses. The MS2 scan of M645 showed a neutral loss of 129 Da (m/z 645 → m/z 516, loss of glutamyl) that is characteristic of glutathione conjugates. This is in agreement with the product ions m/z 372 and 177. The product ion m/z 312 further proved that the glutathione moiety was located on the ethane chain. A γ-hydroxylation was proposed to satisfy the exact mass measurements of the protonated molecules of the metabolites. Similar to the identification of M645, M501 and M516 were proposed as conjugates of mercapturic acid and cysteinyl-glycine, respectively. Their product ion spectra and interpretation of fragmentation are presented in Table 2 and Scheme 5, respectively.

The fragmentations of M629 and M500 (Table 2 and Scheme 5) demonstrated that they were also glutathione and cysteinyl-glycine conjugates, respectively. Their protonated molecules were 16-Da lower than M645 and M516, respectively, indicating that their formation did not involve hydroxylation.

M435 was detected in rat urine in initial survey scan. The exact mass measurement (Table 1) led to the structure assignment as a creatinine conjugate of BM. Further attempts to collect fragmentation and HDX data failed, probably due to poor stability of the metabolite in the matrix.

The survey scan data indicated that M465 still retained both chlorine atoms. This implied that both the chloroethyl moieties were not modified. Upon fragmentation (Table 2 and Scheme 5), M465 underwent a neutral loss of 125.0141 Da which corresponded to the molecular weight of taurine. Hence, M465 was identified as a taurine conjugate of BM on the butyric acid moiety. This proposal is consistent with all further MS3 product ions.

Rat and monkey feces had similar metabolite profiles shown in Figure 2 (rat feces as example). Only M276 and M296 could be identified, along with at least 5 other peaks that were not identified at this time. M368 (m/z 368.1105) was determined to be a metabolite because it shared the same product ion m/z 258.1245 with the known metabolite M322. Likewise, both M352 (m/z 352.1156) and M382 (m/z 382.1624) shared the same fragment ions m/z 260.1403 and m/z 242.1295 that were also generated by the known metabolite M296. Even though their protonated molecules were identified with exact mass measurements, their chemical structures have not been derived thus far. In addition, 2 other minor metabolites at 10.9 and 15.2 min remain totally unknown.

Discussion

The unchanged BM derivative was only detected from very early collections of monkey plasma (0.5–0.75 hr after the start of the 30-minute infusion) and was not detected in any other rat or monkey samples. This indicated that it was rapidly metabolized and/or distributed. Additional *in vitro* incubation of the derivative in control plasma from human, monkey, dog, rat, and mouse indicated that about 90% of that spiked converted to BM in 60 min when incubated in rat and mouse plasma, whereas only about 10% converted in human, monkey, and dog plasma over 3 hr. Therefore, the rapid disappearance of the compound in monkey plasma indicated that distribution may have been predominant.

Despite the observation of many conjugates of BM with cysteine derivatives reported previously, including cysteine, mercapturic acid and thiol, speculated as degradants of initial glutathione conjugates intact glutathione conjugates of BM were only reported in fresh rat urine by this laboratory [1]. The current work led to the identification of more intact glutathione conjugates from rat bile samples, including di-glutathione conjugates, M900 and M916, and single glutathione conjugates M771, M611, M645, and M629. All these glutathione conjugates were not reported previously, and they accounted for a high proportion of the metabolites observed in rat bile, judging from their abundance in the radio chromatogram (Figure 2). In addition, 2 cysteinyl-glycine conjugates of BM (M500 and M516) were also identified from rat bile, and to the best knowledge of the authors, they have not been reported previously. Similar to mercapturic acid conjugates, these cysteinyl-glycine conjugates were also commonly regarded as degradants of initial glutathione conjugates.

Phase II conjugation on the butyric acid moiety for BM has not been reported. The identification of M472A (glucuronic acid conjugation) and M465 (taurine conjugation) from the current investigation revealed that the carboxylic acid group in BM could also undergo conjugation reactions *in vivo*. Although M472A co-eluted with M900 and thereby it is difficult to judge their abundance from the radio chromatogram (Figure 2), the extracted ion chromatogram (data not shown) indicated that it was of the same order of magnitude with M900 as a major metabolite. These 2 metabolites accounted for 18.2% of total radioactivity of the rat bile injection. M465, on the other hand, accounted for 2.2% of the total injected radioactivity (Figure 2).

Since M374 was identified by direct comparison with an authentic synthetic standard, hydroxylation was proposed to

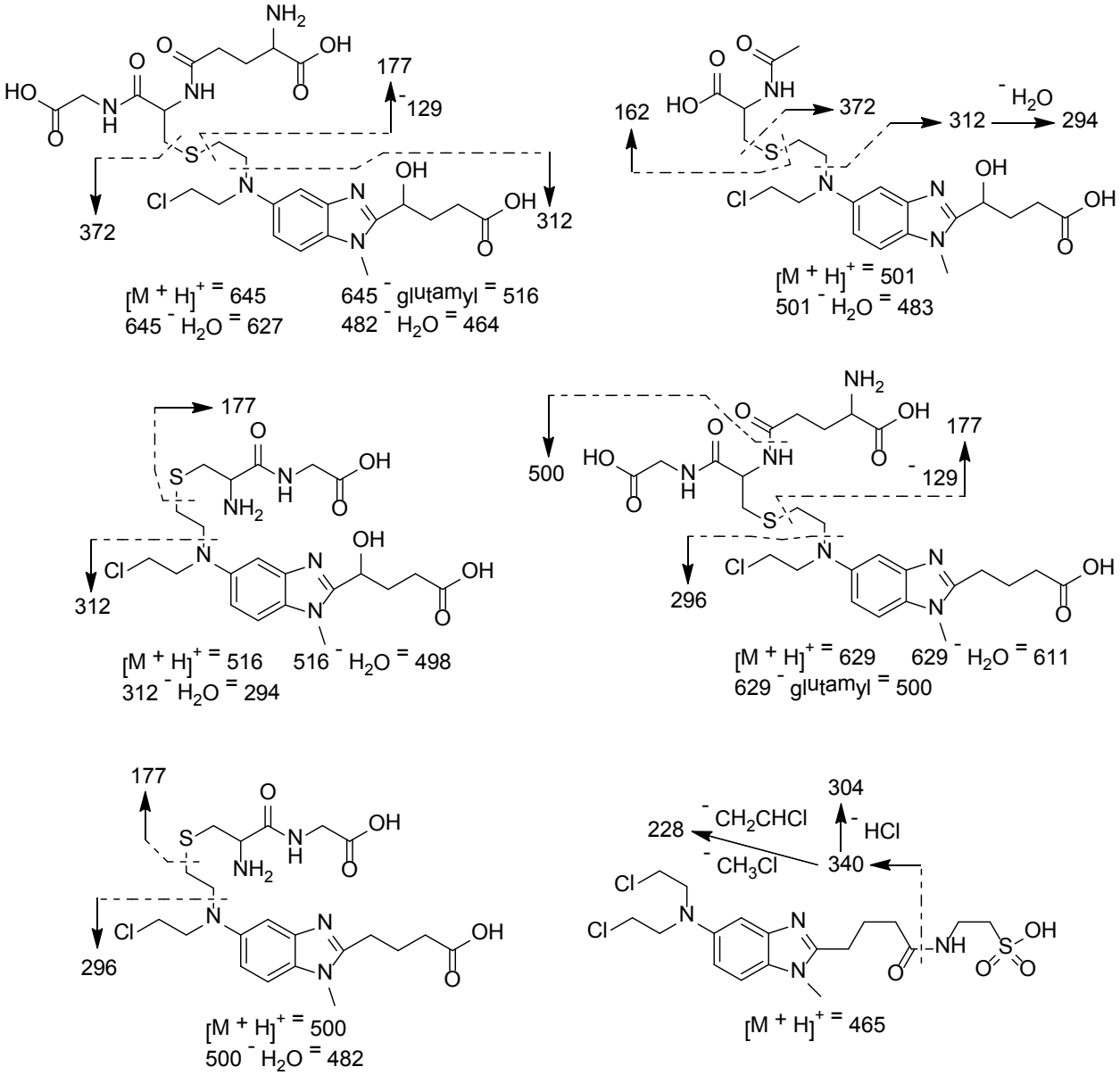

Scheme 5. *Proposed mass spectrometric fragmentation pathways of M645, M501, M516, M629, M500 and M465.*

have occurred to the γ-carbon (C-11) of the butyric acid moiety for M312, M645, M916, and M516. However, M276, M354A, M354B and M336 seemed to suggest that hydroxylation/oxidation also occurred to the chloroethyl moieties.

The methyl group on the benzimidazole moiety was reported to undergo N-demethylation in both rat and human [2-4]. It was also the very first biotransformation of BM observed in human [5,6]. However, in the current study, this biotransformation was not detected in samples obtained from either rat or monkey. Although deemed unlikely, it is not clear if the lack of N-demethylation observed in these studies was caused by the derivatization of BM. Nevertheless, the N-demethylation seemed to be a minor biotransformation anyway in human. When observed, the concentrations of this metabolite (called M4) were more than 2 orders of magnitude lower than the corresponding levels of BM in human [4,7].

Previously, this laboratory reported a BM metabolite with an m/z of 276, which was proposed to have an aldehyde partial structure [1]. In the current study, this metabolite, judged from the product ion spectra, was also detected. After careful analysis of the product ions measured at high resolution (Table 2), it was rationalized to be an imine, instead of the previously proposed aldehyde, as shown in Scheme 2. The key interpretation and rationalization lies in the proposal of mixed formation of isomeric product ions m/z 258, as described in the Results Section. This demonstrated the advantage and power of high resolution exact mass measurements in the field of metabolite identification.

BM conjugates of phosphate, creatinine, and uric acid were reported previously in human urine [4]. In the current study, a phosphate conjugate (M420), a creatinine conjugate (M472B), and uric acid conjugates (M417 and M435) were also detected and identified from rat urine, but not from monkey urine. M435 was only detected in a fresh rat urine sample in initial analysis. It was not detected in the following-up analysis that was designed to collect fragment ion information as well as HDX data. These metabolites co-eluted with other metabolites (Figure 2), so it

is difficult to estimate their relative abundance from the radio chromatograph. However, extracted ion chromatograms of these metabolites indicated they were all minor metabolites, about 1 order of magnitude lower than the major metabolites such as M900.

The proposal of M260 represents a novel intra molecular nucleophilic/electrophilic mechanism for BM that has not been reported before. The abundance in the radio chromatogram (Figure 2) indicates that this is one of the major metabolism pathways of BM and/or its derivative in monkey.

Conclusion

In conclusion, the novel BM derivative was rapidly metabolized in rat and monkey to generate almost exclusively BM and BM-related metabolites. These metabolites indicated that the overall biotransformation pathways are similar to those reported previously for BM, including primarily direct conjugation with glutathione, cysteine derivatives, chlorine-carbon bond hydrolysis, γ-hydroxylation on the butyric acid moiety, and hydroxylation/oxidation on the mechlorethamine moiety. New biotransformation pathways were also discovered, including aziridine formation on the mechlorethamine moiety that was postulated due to intra-molecular nucleophilic attack of the electrophilic carbon atom (connecting chlorine) by the amino nitrogen atom, as well as the phase II conjugation on the butyric acid functionality with glucuronic acid and taurine. In spite of the variety of BM metabolites identified from rat and monkey excreta, N-demethylation, forming a relatively minor circulating metabolite in humans, was not detected.

Acknowledgment

The work was funded by Teva Branded Pharmaceutical Products R&D, Inc.

Disclosure statement

The authors report no conflicts of interest.

References

1. Cugati S, Wang JJ, Knudtson MD, et al. Retinal vein occlusion and vascular mortality: Pooled data analysis of 2 population-based cohorts. Ophthalmology. 2007;114:520-4.
2. Chovan JP, Li F, Yu E, et al. Metabolic profile of [14C] bendamustine in rat urine and bile: Preliminary structural identification of metabolites. Drug Metab Dispos. 2007;35:1744-53.
3. Teichert J, Sohr R, Baumann F, et al. Synthesis and characterization of some new phase II metabolites of the alkylator bendamustine and their identification in human bile, urine, and plasma from patients with cholangiocarcinoma. Drug Metab Dispos. 2005;33:984-92.
4. Teichert J, Sohr R, Hennig L, et al. Identification and quantitation of the N-acetyl-L-cysteine S-conjugates of bendamustine and its sulfoxides in human bile after administration of bendamustine hydrochloride. Drug Metab Dispos. 2009;37:292-301.
5. Dubbelman AC, Jansen RS, Rosing H, et al. Metabolite profiling of bendamustine in urine of cancer patients after administration of [14C] bendamustine. Drug Metab Dispos. 2012;40:1297-1307
6. Matthias M, Preiss R, Sohr R, et al. Pharmacokinetics of bendamustine in patients with malignant tumors (Abstract). Proc Annu Meet Am Soc Clin Oncol. 1995;14:1476.
7. Preiss R, Matthias M, Merkle KH. Pharmacological and clinical data of bendamustine. In: Proceedings of the 17th International Cancer Congress. 1998;1637-40.

***Correspondence to:**

Austin C. Li
Drug Metabolism and Pharmacokinetics
Teva Pharmaceuticals Specialty R&D, Inc.
West Chester, PA-19380
USA
Tel: +610 883 5616
E-mail: Austin.li@tevapharm.com